Invited Paper

Advantages of Interaction-Based Readout for Quantum Sensing

Emily Davis, Gregory Bentsen, Tracy Li, and Monika Schleier-Smith

Stanford University Physics Department, 382 Via Pueblo Mall, Stanford CA, U.S.A

ABSTRACT

Detection noise poses a challenge for achieving Heisenberg-limited phase estimation. We discuss a "twisting echo" protocol[1] that addresses this problem by using interactions to amplify a spectroscopic signal. The echo protocol enables phase sensitivity near the Heisenberg limit while permitting detection noise on the order of the quantum noise of an unentangled state. For comparison with conventional schemes requiring direct detection of entangled states, we calculate the dependence of metrological gain on detection noise in Ramsey spectroscopy with squeezed, twin Fock, and GHZ states. The twisting echo outperforms all of these alternatives if the detection uncertainty is at or above the single-atom level.

Keywords: metrology, entanglement, atomic physics, quantum information

1. INTRODUCTION

Developments in quantum metrology have enabled increasingly precise sensors, with envisioned applications ranging from navigation to measurements of fundamental constants. Such sensors determine the energy difference $\hbar\omega$ between two quantum states, $|\downarrow\rangle$ and $|\uparrow\rangle$, by measuring a phase $\phi = \omega T$ accumulated during an interrogation time T. Making N uncorrelated measurements, or measuring N uncorrelated quantum systems, allows a statistical uncertainty as low as $\Delta\phi = 1/\sqrt{N}$, which is called the standard quantum limit (SQL). However, the use of entangled states in principle allows phase detection at the absolute lower bound imposed by quantum mechanics, the Heisenberg limit (HL) $\Delta\phi = 1/N$.

Significant effort has been expended to engineer entangled quantum states that can circumvent the SQL on phase detection. Historically, experiments have principally focused on squeezed states,[2–10] which have already enhanced the precision of clocks, magnetometers, and atom interferometers. Experiments have also realized more exotic non-Gaussian entangled states,[11,12] in principle allowing phase sensitivity approaching the fundamental Heisenberg limit. However, detection noise limits the actual metrological gain achieved in traditional schemes requiring direct state detection. In particular, single-particle detection resolution is required to reach the Heisenberg limit. Such high resolution is difficult to attain at large particle number,[13,14] where the potential metrological gain is highest. An emerging alternative is to design interactions that amplify the spectroscopic signal prior to state detection.[1,15–17]

In Ref. [1], we proposed an interaction-based "twisting echo" protocol that attains near-Heisenberg-limited phase resolution while permitting detection noise $\sim \sqrt{N}$. Our procedure employs the one-axis twisting Hamiltonian[18] to transform a coherent spin state into an intermediate entangled state, which is then perturbed. In order to amplify the perturbation, the sign of the Hamiltonian is switched to "untwist" into a displaced version of approximately the original state. In this manuscript, we reiterate the salient details of the original proposal and explicitly compare it to traditional direct detection methods on a set of metrologically relevant states. We discuss the advantages of the twisting echo with respect to requirements on coherent evolution time, detection noise tolerance, and dynamic range.

Further author information: (Send correspondence to Emily Davis)
Emily Davis: E-mail: emilyjd@stanford.edu, Telephone: 1 650 497 4061

Advances in Photonics of Quantum Computing, Memory, and Communication X, edited by Zameer Ul Hasan, Philip R. Hemmer, Hwang Lee, Alan L. Migdall, Proc. of SPIE Vol. 10118, 101180Z
 · doi: 10.1117/12.2257033

2. QUANTUM METROLOGY WITH NOISY DETECTION

To illustrate the challenge posed by detection noise, we discuss the bound on the metrological precision when detecting states of known metrological relevance with and without noise. We model our system as an ensemble of N two-level systems with basis (pseudo)spin states $|\downarrow\rangle, |\uparrow\rangle$. We define the collective spin vector $\mathbf{S} \equiv \sum_{i=1}^{N} \mathbf{s_i}$ and consider pure states within the permutation-symmetric space, with basis states $|S, m\rangle$ of total angular momentum $S = N/2$ and S_z-projection m, with $-S \leq m \leq S$. We assume we can make projective measurements of $S_z = (n_\uparrow - n_\downarrow)/2$, where $n_\uparrow, n_\downarrow$ are the populations of the two spin states.

After initializing a pure state $\rho(0) = |\psi_0\rangle\langle\psi_0|$, we allow it to precess by an angle ϕ about an axis $\vec{n}$, obtaining $\rho(\phi) = e^{-i\phi S_n}\rho_0 e^{i\phi S_n}$, where ϕ is the quantity of interest. Given the problem of phase estimation, the standard protocol is to projectively measure $\rho(\phi)$ and build up a distribution $f(m;\phi) = \langle m|\rho(\phi)|m\rangle$, from which $\rho(\phi)$ and thus ϕ can be extrapolated. We call this procedure "direct detection." Sample S_z distributions that would be acquired using perfect, noiseless direct detection are shown in Fig. 1 for the following states of interest:

2.0.1 Coherent Spin States

The simplest useful state for metrology is the unentangled coherent spin state (CSS) satisfying

$$S_{\theta,\varphi}|\theta,\varphi\rangle = S|\theta,\varphi\rangle, \tag{1}$$

where $S_{\theta,\varphi} = S_x\sin(\theta)\cos(\varphi) + S_y\sin(\theta)\sin(\varphi) + S_z\cos(\theta)$. The Wigner function (Fig. 1a) shows the intrinsic quantum spin noise equalized between quadratures $\langle\Delta S_y^2\rangle = \langle\Delta S_z^2\rangle = 1/2|\langle S_x\rangle| = S/2$. Rotations $e^{-i\phi S_y}$ of $|\pi/2, 0\rangle$ can be detected with at best a phase resolution

$$\Delta\phi = \left[\frac{\Delta S_z}{\partial_\phi\langle S_z\rangle}\right]_{\phi=0} = \frac{\sqrt{S/2}}{S} = \frac{1}{\sqrt{N}} \tag{2}$$

where $\langle S_z\rangle$ and ΔS_z and represent the mean and standard deviation of S_z and $\partial_\phi \equiv d/d\phi$.

2.0.2 Squeezed and Oversqueezed States

Squeezed spin states, so named for their redistributed quantum noise, have been generated with both the one-axis twisting Hamiltonian[4,7,19,20] $H_{\text{twist}} = \chi S_z^2$ and quantum non-demolition measurements.[9,10,21] The squeezed states produced by one-axis twisting can be parameterized by the "twisting strength" $Q \equiv 2S\chi t$. The metrologically optimal squeezed state[18] for H_{twist} is obtained at $Q_{sq} = \sqrt[6]{24}S^{1/3}$:

$$|\psi_{sq}\rangle = e^{-iQ_{sq}Sz^2/(2S)}|\pi/2, 0\rangle \tag{3}$$

The Wigner function (Fig. 1b) reveals the decreased standard deviation $\Delta S_{sq} = \sqrt{\frac{1}{2}(\frac{S}{3})^{1/3}}$ in one quadrature, at the price of increased variance in the other. Rotations of a squeezed state $|\psi_{sq}\rangle$ can be detected with phase resolution $\Delta\phi = \left[\Delta S_{sq}/\partial_\phi\langle S_z\rangle\right]_{\phi=0}$. Thus, we clearly benefit from the decreased standard deviation ΔS_{sq}.

At greater twisting strength $Q > Q_{sq}$, the state becomes non-Gaussian, and the squeezing no longer captures the full metrological potential of the entangled state.[22] In particular, the non-Gaussian oversqueezed state obtained at $Q \approx \sqrt{2S}$ (Fig. 1c) provides an even higher metrological gain than the optimally squeezed state in the twisting echo protocol, to be described in Sec. 3.

2.0.3 Dicke States

Dicke states are defined as the eigenstates of the S_z operator $S_z|m\rangle = m|m\rangle$. Here we focus on a special case, the twin Fock state $|0\rangle \equiv |S = N/2, m = 0\rangle$, because it has the highest potential metrological gain of all Dicke states, as quantified by the quantum Fisher information (Sec 2.1). This state has been realized experimentally.[12] It is non-Gaussian, as is evident from the Wigner function and the S_z distribution (Fig. 1d). Therefore, detecting a rotation $e^{-i\phi S_y}$ of $|0\rangle$ is no longer straightforward. Certainly we are no longer interested in mean $\langle S_z\rangle$, which we

used for the CSS and the squeezed states, because $\partial_\phi \langle S_z \rangle |_{\phi=0} = 0$ for $|0\rangle$. Apellaniz et al.[23] have shown that a convenient observable is the variance ΔS_z^2. For small ϕ, measuring ΔS_z^2 yields a phase sensitivity

$$\Delta\phi = \left[\frac{\Delta S_z^2}{\partial_\phi \langle S_z^2 \rangle}\right]_{\phi=0} = \sqrt{\frac{1}{2S(S+1)}}. \tag{4}$$

Thus, in the large-N limit, the Dicke state ideally achieves a phase uncertainty only a factor $\sqrt{2}$ above the Heisenberg limit, $\Delta\phi \approx \sqrt{2}/N$.

2.0.4 GHZ States

Finally, we discuss the non-Gaussian GHZ (Schrödinger's cat) states $|\psi_{GHZ}\rangle = (|-S\rangle + |S\rangle)/\sqrt{2}$, which have been realized with up to 14 ions.[11] Bollinger et al.[17] discuss how ϕ can be extracted for GHZ states by measuring the parity $\tilde{\Pi} \equiv \Pi_{i=1}^{N} s_{z,i}$, which gives

$$\Delta\phi = \frac{\Delta\tilde{\Pi}}{\partial_\phi \langle \tilde{\Pi} \rangle} = 1/N. \tag{5}$$

Due to the periodicity of the GHZ state, evident in the Wigner function in Fig. 1e, the dynamic range of phase detection is limited to small angles $\phi \lesssim 1/N$. Schemes have been proposed to solve this problem by simultaneously interrogating multiple GHZ states of varying atom number.[24]

2.1 Fisher Information and the Cramér-Rao Bound

Having introduced a set of metrologically interesting states, we would like to capture their metrological "usefulness" using a simple metric. In classical probability theory, the Fisher information quantifies the information about an unknown parameter ϕ that can be extracted from a measurements of a random variable ξ with probability distribution $f(\xi;\phi)$. It can be written as

$$F(\phi) = \int d\xi \frac{1}{f(\xi|\phi)} \left(\frac{\partial f(\xi|\phi)}{\partial\phi}\right)^2. \tag{6}$$

For any unbiased estimator $\hat{\phi}$ of ϕ, the Fisher information satisfies $\mathrm{Var}[\hat{\phi}] \geq 1/F(\phi)$, thus placing a bound on the precision of any estimate of ϕ.

By extension, Braunstein and Caves[25] have defined the quantum Fisher information (QFI) of a general density matrix ρ. For a pure state of the form $\rho(\phi) = e^{-i\phi S_n} |\psi_0\rangle \langle\psi_0| e^{i\phi S_n}$, we can rewrite the QFI simply as

$$F_Q(\rho(0), S_n; \phi) = 4\mathrm{Var}[S_n] \tag{7}$$

Selecting the rotation axis judiciously for a given inital $\rho(0)$ maximizes Eq. 7; the result is called the quantum Cramér-Rao bound (QCRB). It is important to select the correct rotation axis in order to benefit metrologically from the state; to emphasize this point, we plot the QFI as a function of rotation axis for each state (Fig. 1). After determining the correct rotation axis, we calculate the quantum Cramér-Rao bound for each state of interest and corresponding minimum $\Delta\phi$ in the large N limit (Table 1). The phase sensitivity is related to the QFI by

$$\Delta\phi = \frac{1}{\sqrt{F_Q(\rho(0), S_n; \phi)}} \geq \frac{1}{\sqrt{QCRB}} \tag{8}$$

Thus, we see that QCRB$> N$ corresponds to phase sensitivity beyond the SQL, and consequently implies entanglement. Indeed, QCRB$> kN$ requires k-particle entanglement,[26] up to a maximum of QCRB $= N^2$ corresponding to N-particle entanglement. We quantify the resulting metrological gain by $1/N\Delta\phi^2 = \mathrm{QCRB}/N$, which compares the QCRB of any given quantum state to that of a CSS.

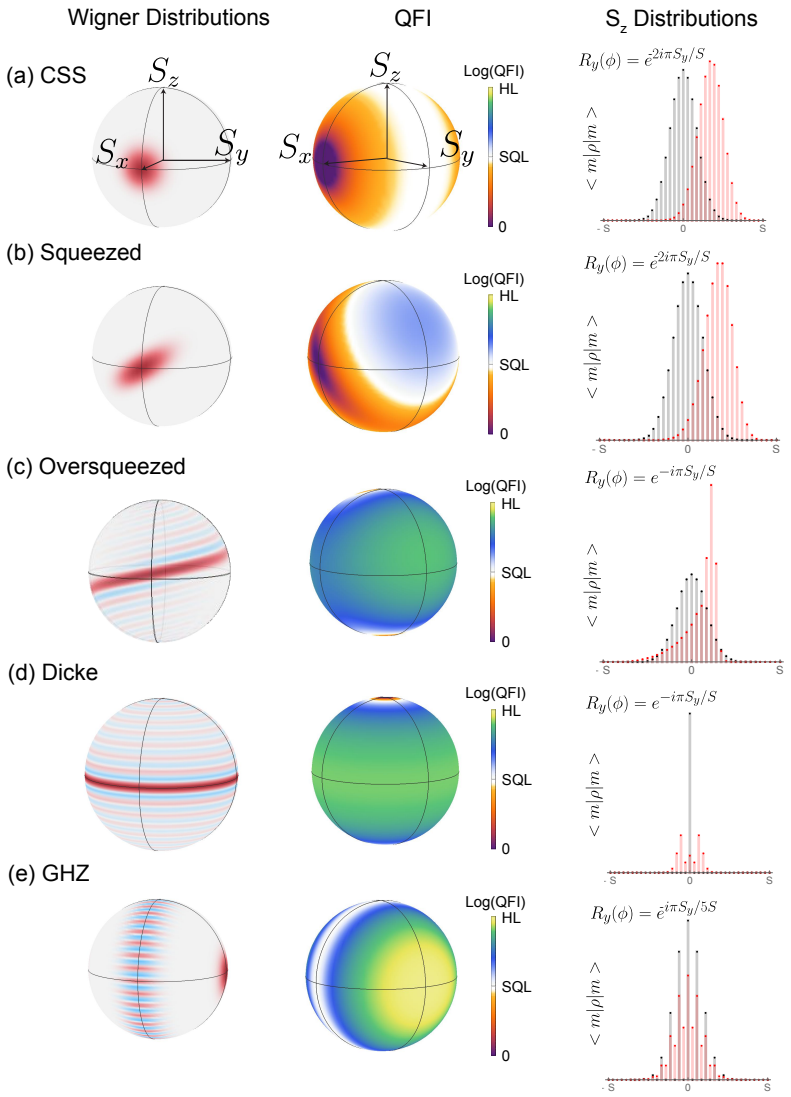

Figure 1. First column: Wigner quasiprobability distributions on the Bloch sphere for five states of interest, with $N = 36$ atoms. The Wigner function reveals the structure of each state, thus yielding intuition about the optimal rotation axis. Second column: The QFI is plotted for each state. (Note that the Bloch spheres in the second column are rotated with respect to those in the first column.) The surface color corresponds to Log(QFI) about an axis through each point θ, φ on the Bloch sphere. We can verify that the axes corresponding to the QCRB match the intuition we gain from the Wigner function. For example, rotating the twin Fock state $|0\rangle$ about the z axis yields no information. The QFI of the GHZ state is greater than or equal to the SQL about all axes. Third column: S_z distributions obtained from noiseless direct state detection for the unrotated state $\rho(0)$ (black) and rotated state $\rho(\phi)$ (red).

2.2 Decrease of Metrological Gain with Detection Noise

Thus far we have assumed perfect detection, but in any experiment, the actual metrological gain is degraded by detection noise. The adverse effect is particularly severe for non-Gaussian states[22] because the actual distribution must be resolved instead of the shift of an average value. To model the effect of detection noise on the Cramér-Rao bound for each state, we take the original pure state S_z distribution $f(m) = \langle m|\rho(0)|m\rangle$ and convolve it with a Gaussian noise distribution of width $\Delta S_{meas} = \Delta n/2$, where Δn is the particle number resolution. This

yields a probability distribution

$$f(m;\Delta S_{meas}) = \int_{x=-S}^{S} \langle m|\rho|m\rangle \, e^{-(x-m)^2/2\Delta S_{meas}^2} dx \tag{9}$$

which we use to calculate the Cramér-Rao bound as a function of ΔS_{meas}. Sample S_z distributions for different values of detection noise are plotted in Fig. 2.

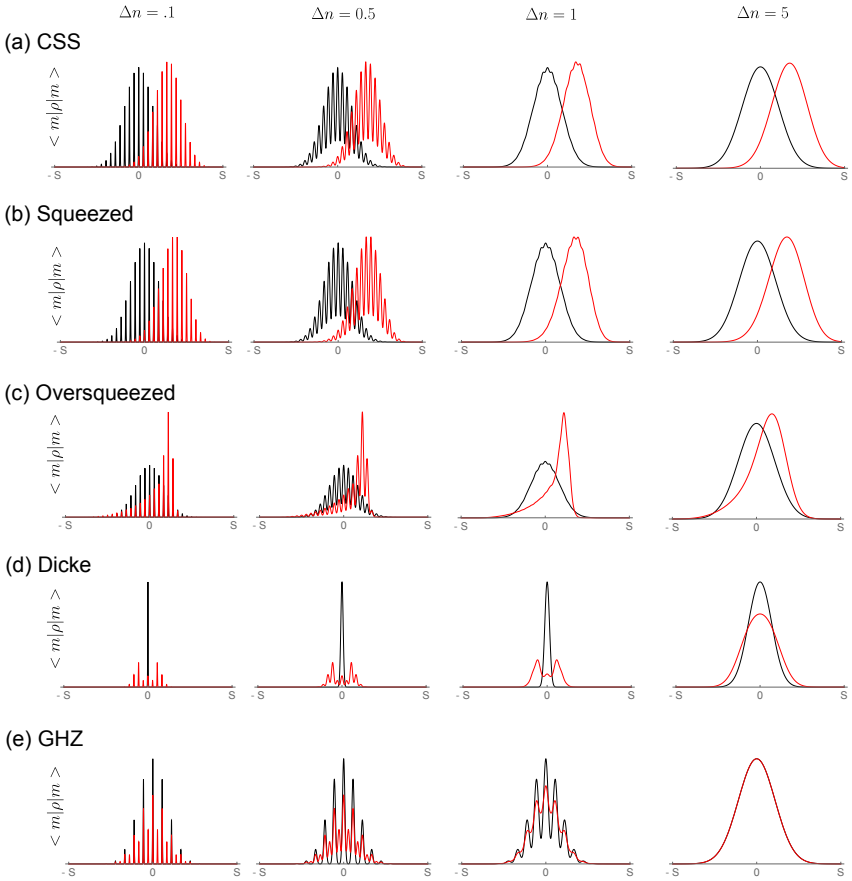

Figure 2. Sample S_z distributions for the same states $\rho(0)$ (black) and $\rho(\phi)$ (red) displayed in the third column of Fig. 1, for $N = 36$ atoms. The detection noise increases from left to right, with particle resolution $\Delta n = 0.1, 0.5, 1$, and 5. The noise has no effect on the signal for the coherent and squeezed spin states, because the shifted mean $\langle S_z\rangle$ is preserved. However, the noise destroys the signal for the non-Gaussian states.

We quantify the loss of phase resolution by plotting the metrological gain as a function of particle resolution $\Delta n = 2\Delta S_{meas}$ for each state in Fig. 3. The higher the CRB at perfect detection, the more quickly the CRB degrades as Δn increases. For example, the GHZ state reaches the Heisenberg limit only if we can detect with single-particle resolution $\Delta n \ll 1$. This demanding requirement raises the question: is there a way to benefit from entanglement without perfect detection?

3. TWISTING ECHO

In Ref. [1], we proposed a "twisting echo" protocol designed to enable phase resolution near the Heisenberg limit while only requiring a detection resolution comparable to the CSS noise. Starting with a CSS $|\pi/2, 0\rangle$, (Fig. 4a),

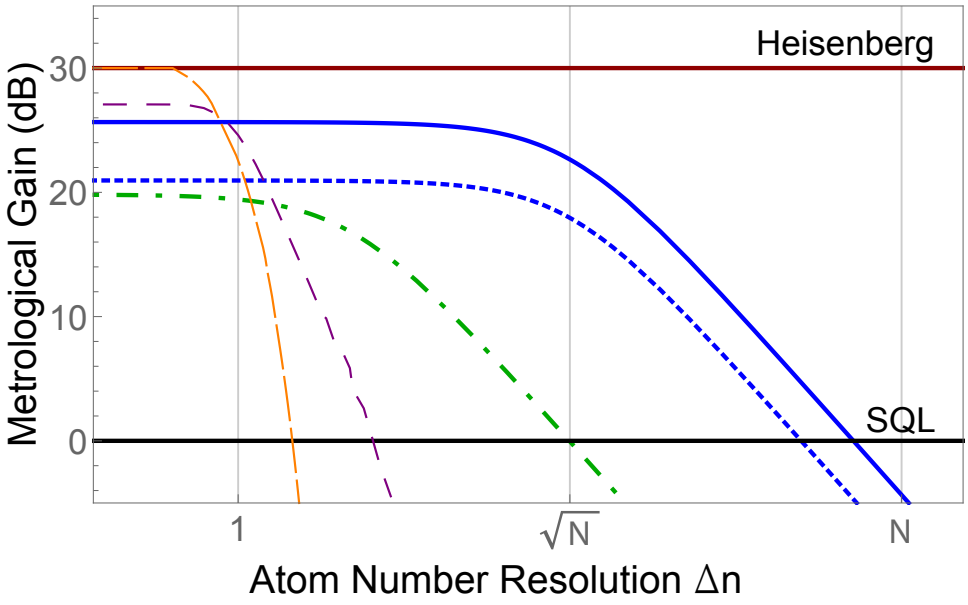

Figure 3. Metrological gain *vs.* measurement uncertainty Δn for direct detection of the squeezed state at Q_{sq} (dot-dashed green), the Dicke state $|0\rangle$ (dashed purple), and the GHZ state $R_y(\phi)(|\pi/2,\pi/2\rangle+|\pi/2,-\pi/2\rangle)$ (dashed orange), compared to performance of the twisting echo introduced in Sec. 3 with twisting strength Q_{opt} (solid blue) or Q_{sq} (dotted blue).

Table 1. We collect the important metrological information about the states defined in Sections 2.0.1 - 2.0.4.

State	CRB	$\Delta\phi$, large N limit
CSS	2S	$N^{-1/2}$
Squeezed state $\|\psi_{sq}\rangle$	$\sqrt[3]{24}S^{5/3}$	$\sqrt[6]{\frac{4}{3}}N^{-5/6}$
Dicke $\|0\rangle$	$2S(S+1)$	$\sqrt{2}N^{-1}$
GHZ	$4S^2$	N^{-1}

we apply the twisting Hamiltonian $H_{\text{twist}} = \chi S_z^2$ for a time t to obtain an entangled state $|\psi_e\rangle = U\,|\pi/2,0\rangle$, where $U = e^{-i\chi S_z^2 t}$ (Fig. 4b). We wish to use this state to sense a rotation about the $\hat{\mathbf{y}}$ axis. The rotation $R_y(\phi) = e^{-i\phi S_y}$ shifts the state upwards, as indicated in Fig. 4c. Finally, we reverse the twisting by evolving for time t with a Hamiltonian of the opposite sign, $H_{\text{twist}} = -\chi S_z^2$. Because the center of the state $|\psi_e\rangle$ was shifted above $S_z = 0$ by the rotation (Fig. 4c), the S_z dependent "untwisting" action shifts the average spin projection $\langle S_y\rangle$ leftwards (Fig. 4d). We thus obtain a final state $U^\dagger R_y(\phi)U\,|\pi/2,0\rangle$ with $\langle S_y\rangle$ shifted in proportion to ϕ, but with roughly the same noise as the original CSS (Fig.4d).

The phase resolution is given by

$$\Delta\phi = \left[\frac{\Delta S_y^\phi}{\partial_\phi \langle S_y^\phi\rangle}\right]_{\phi=0} \tag{10}$$

where $\langle S_y^\phi\rangle$ and ΔS_y^ϕ represent the mean and standard deviation of S_y after the echo. We calculate in [1] that at $Q_{opt} \approx \sqrt{N}$, corresponding to the "oversqueezed" state in Fig. 4b, the twisting echo attains Heisenberg scaling of the phase resolution,

$$\Delta\phi_{\text{min}} = \sqrt{e}/N. \tag{11}$$

Qualitatively, the "untwisting" step in the echo sequence offers two benefits. Firstly, by transferring the phase information to the average displacement of a near-Gaussian state, it makes the signal easier to detect and

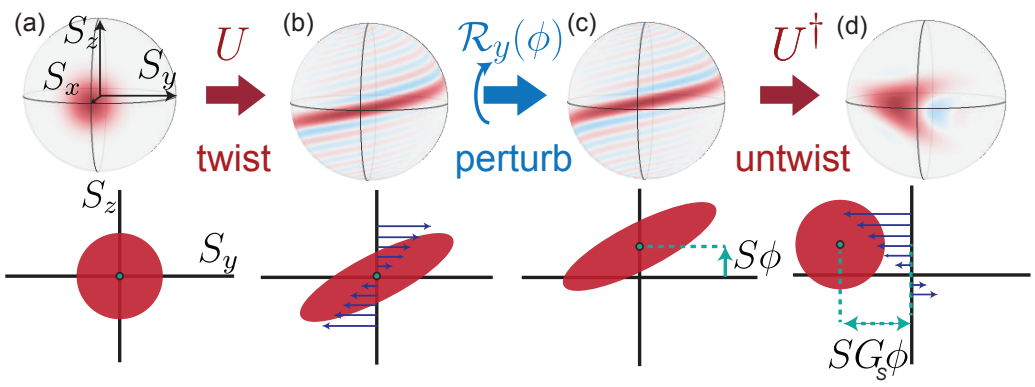

Figure 4. Twisting echo for entanglement-enhanced measurement. Top row: The initial CSS $|\pi/2, 0\rangle$ (a) evolves under H_{twist} into an oversqueezed state $|\psi_e\rangle$ (b). To detect a rotation of $|\psi_e\rangle$ about $\hat{y}$ by a small angle ϕ (b $\to$ c), we amplify the perturbation into a large displacement by applying $-H_{\text{twist}}$ (c$\to$d). Illustrated are Wigner quasiprobability distributions for 2S = 30 atoms, with $\phi = 1/S$. Bottom row: Cartoon depiction of the same steps, with blue flow lines indicating twisting and untwisting.

increases the detection noise tolerance. Secondly, it actually improves upon the signal-to-noise ratio (SNR) of the intermediate entangled state. Both effects are shown in Fig. 3.

To illustrate the benefits of the untwisting concretely, we explicitly compare the signal and noise of the optimally squeezed state with $Q_{sq} = \sqrt[6]{24}S^{1/3}$ to the signal and noise of the twisting echo with Q_{sq}. (We use Q_{sq} for this example even though it is not optimal for the echo protocol, because once we twist beyond the Gaussian squeezed state to the oversqueezed state, or any other non-Gaussian state, it is no longer meaningful to consider the signal and noise independently.) The signal of the twisting echo is enhanced compared to the squeezed state signal, $S\phi$, by a factor

$$G_S \equiv (2S-1)\sin(Q/2S)\cos^{2S-2}(Q/2S) \tag{12}$$

which in the large N limit and at Q_{sq} reduces to $G_S = \sqrt[6]{24}S^{1/3}$.[1] The noise of the twisting echo $\Delta S_y^\phi \sim \sqrt{S/2}$, is increased compared to the squeezed state noise, $\Delta S_{sq} = \sqrt{\frac{1}{2}(\frac{S}{3})^{1/3}}$, by a factor

$$G_N \equiv \frac{\Delta S_y^\phi}{\Delta S_{sq}} = \sqrt[6]{3}S^{1/3} \tag{13}$$

The signal gain G_S is a factor of $\sqrt[6]{8}$ greater than the noise gain G_N. We have therefore increased the SNR while simultaneously making our signal much easier to detect. While the improvement in SNR is only a constant factor for the squeezed state, the optimal oversqueezed state improves the scaling of the metrological gain with atom number to reach the Heisenberg scaling in Eq. 11.

Squeezed and oversqueezed states are not the only ones that may benefit from use of the echo protocol. In principle, one can prepare a GHZ state by applying the twisting Hamiltonian for $Q_{GHZ} = \pi N/2$, perturb it, untwist, and measure the coherent state displacement. The "GHZ echo" sequence, similar to a protocol described in Ref. [17], obtains Heisenberg-limited measurement precision with noise tolerance $\Delta n \sim N$, at the price of requiring a very long coherent evolution time $2Q_{GHZ} = \pi N$. Remarkably, the optimal twisting echo also achieves Heisenberg scaling of the phase sensitivity, but in an evolution time that is shorter by a factor $\sim \sqrt{N}$ (Fig. 5).

3.1 Dynamic Range

Entanglement-enhanced phase resolution typically comes at the price of a reduction in dynamic range (Sec. 2.0.4). To investigate this tradeoff for the twisting echo, we plot the metrological gain as a function of twisting strength Q and rotation angle ϕ for a final state $e^{Q/2S}R_y(\phi)e^{-Q/2S}|\pi/2, 0\rangle$ in Fig. 6, for $N = 10^3$ atoms. The metrological gain of the twisting echo is highest at Q_{opt} for small $\phi \sim 1/N$ but decreases by only 6 dB at $\phi \sim 1/\sqrt{N}$. By contrast, the dynamic range of a GHZ state is limited to $\phi \lesssim 1/N$. The twisting echo provides the flexibility to choose an optimal twisting strength Q according to the expected maximum phase perturbation.

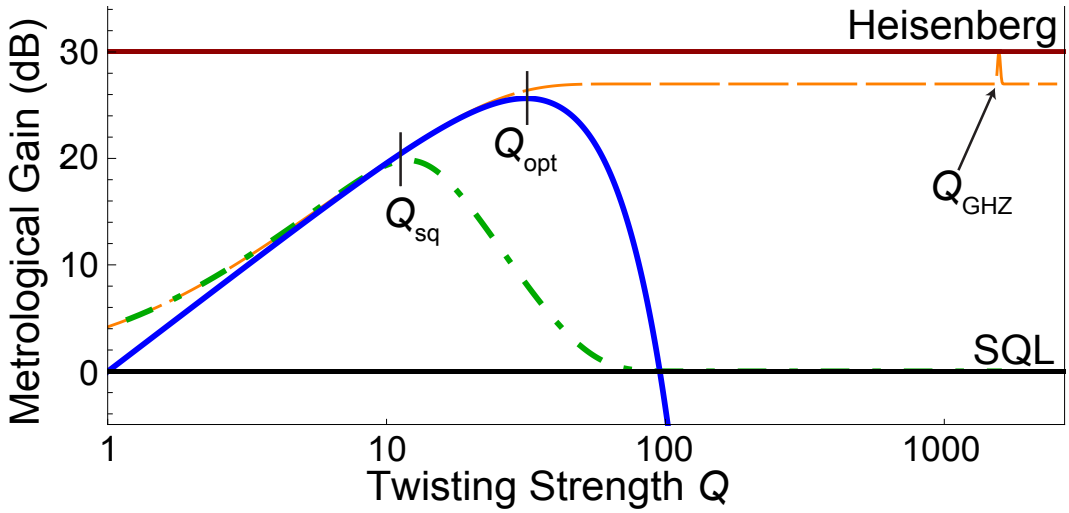

Figure 5. Metrological gain *vs* twisting strength Q with $N = 10^3$ atoms for the unitary twisting echo (solid blue), compared to spin squeezing (dot-dashed green) and the quantum Cramér-Rao bound (QCRB) on phase sensitivity (dashed orange). Horizontal lines indicate the standard quantum limit (black) and Heisenberg limit (red). The twisting echo nearly follows the QCRB to its plateau at $Q \approx \sqrt{N}$; only at a much longer time $Q_{GHZ} = N\pi/2$ does the QCRB increase by 3 dB to reach the Heisenberg limit. Attaining Heisenberg-limited phase sensitivity by the "GHZ echo" requires requires extra rotations compared with the twisting echo $U^\dagger R_y(\phi) U \left|\pi/2, 0\right\rangle$ considered here, which is why the blue curve does not reach the HL at Q_{GHZ}.

4. OUTLOOK

We have demonstrated two advantages of the twisting echo method: the short evolution time to reach Heisenberg scaling and the high tolerance to detection noise. Notably, these features compare favorably to the long evolution time and low detection noise required to reach the Heisenberg limit using GHZ states. Furthermore, the dynamic range of the twisting echo can be tuned to provide significant metrological gain for sensing comparatively large rotations. We emphasize that interaction-enhanced readout can be applied broadly, if the scheme is tailored to the system at hand. For example, a modified scheme applicable to squeezed states, requiring only a single sign of interactions, has recently been demonstrated by Hosten et al.[15] Promising platforms for harnessing non-Gaussian oversqueezed states to approach the Heisenberg limit include ion traps, where oversqueezing and switchable-sign interactions have already been realized;[20,27] or neutral atoms interacting via a strong-coupling cavity[1] or by Rydberg dressing.[28] For applications of these systems to optical clocks, it may prove useful to explore cascaded schemes similar to Ref. [24], where the tunable dynamic range of the twisting echo could aid in combining the benefits of entanglement and long interrogation time.

ACKNOWLEDGMENTS

This work was supported by the AFOSR, the Alfred P. Sloan Foundation, the NSF, the Fannie and John Hertz Foundation, and the Hellman Fellows Fund.

REFERENCES

[1] Davis, E., Bentsen, G., and Schleier-Smith, M., "Approaching the Heisenberg limit without single-particle detection," *Physical Review Letters* **116**, 053601 (2016).

[2] Leroux, I. D., Schleier-Smith, M. H., and Vuletic, V., "Orientation-dependent entanglement lifetime in a squeezed atomic clock," *Physical Review Letters* **113**, 103004 (2014).

[3] Wasilewski, W., Jensen, K., Krauter, H., Renema, J. J., Balabas, M. V., and Polzik, E. S., "Quantum noise limited and entanglement-assisted magnetometry," *Physical Review Letters* **113**, 133601 (2010).

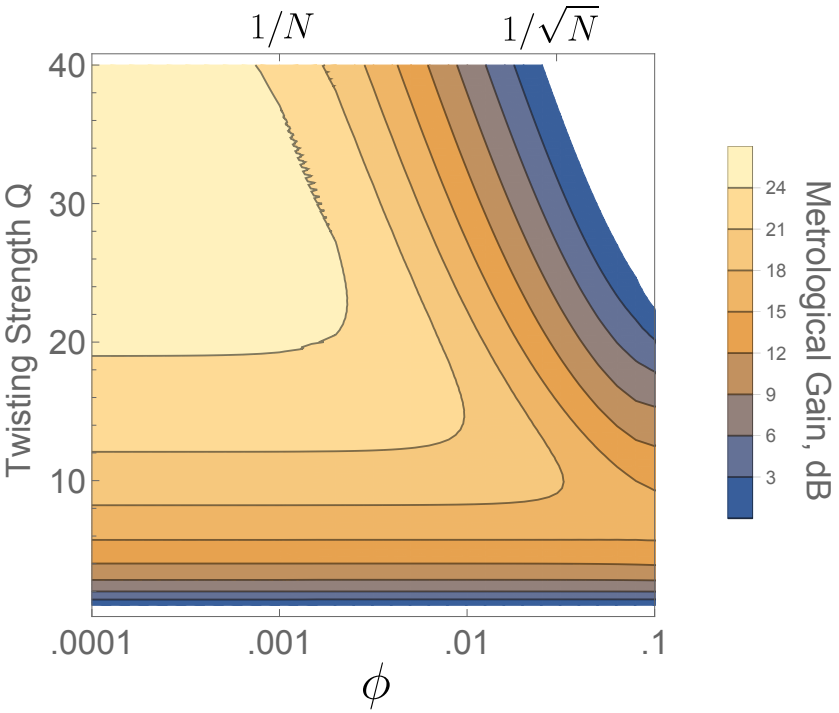

Figure 6. Metrological gain of the twisting echo with $N = 10^3$ atoms, as a function of twisting strength Q and rotation angle ϕ. While the metrological gain is maximal at Q_{opt} and small $\phi \sim 1/N$, a higher dynamic range can be obtained by choosing lower Q, at the price of slightly decreased metrological gain.

[4] Gross, C., Zibold, T., Nicklas, E., Estéve, J., and Oberthaler, M. K., "Nonlinear atom interferometer surpasses classical precision limit," *Nature* **464**, 1165–1169 (2010).

[5] Hamley, C. D., Gerving, C., Hoang, T., Bookjans, E., and Chapman, M. S., "Spin-nematic squeezed vacuum in a quantum gas," *Nature Physics* **8**(4), 305–308 (2012).

[6] Sewell, R., Koschorreck, M., Napolitano, M., Dubost, B., Behbood, N., and Mitchell, M., "Magnetic sensitivity beyond the projection noise limit by spin squeezing," *Physical Review Letters* **109**(25), 253605 (2012).

[7] Ockeloen, C. F., Schmied, R., Riedel, M. F., and Treutlein, P., "Quantum metrology with a scanning probe atom interferometer," *Physical Review Letters* **111**(14), 143001 (2013).

[8] Muessel, W., Strobel, H., Linnemann, D., Hume, D., and Oberthaler, M., "Scalable spin squeezing for quantum-enhanced magnetometry with Bose-Einstein condensates," *Physical Review Letters* **113**, 103004 (2014).

[9] Bohnet, J. G., Cox, K. C., Norcia, M. A., Weiner, J. M., Chen, Z., and Thompson, J. K., "Reduced spin measurement back-action for a phase sensitivity ten times beyond the standard quantum limit," *Nature Photonics* **8**(9), 731–736 (2014).

[10] Hosten, O., Engelsen, N. J., Krishnakumar, R., and Kasevich, M. A., "Measurement noise 100 times lower than the quantum-projection limit using entangled atoms," *Nature* **529**, 505–508 (2016).

[11] Monz, T., Schindler, P., Barreiro, J. T., Chwalla, M., Nigg, D., Coish, W. A., Harlander, M., Hänsel, W., Hennrich, M., and Blatt, R., "14-qubit entanglement: Creation and coherence," *Physical Review Letters* **106**, 130506 (2011).

[12] Lücke, B., Scherer, M., Kruse, J., Pezzè, L., Deuretzbacher, F., Hyllus, P., Peise, J., Ertmer, W., Arlt, J., Santos, L., Smerzi, A., and Klempt, C., "Twin matter waves for interferometry beyond the classical limit," *Science* **334**, 773–776 (2011).

[13] Zhang, H., McConnell, R., Ćuk, S., Lin, Q., Schleier-Smith, M. H., Leroux, I. D., and Vuletić, V., "Collective state measurement of mesoscopic ensembles with single-atom resolution," *Physical Review Letters* **109**, 133603 (2012).

[14] Hume, D. B., Stroescu, I., Joos, M., Muessel, W., Strobel, H., and Oberthaler, M. K., "Accurate atom counting in mesoscopic ensembles," *Physical Review Letters* **111**, 253001 (2013).

[15] Hosten, O., Krishnakumar, R., Engelsen, N. J., and Kasevich, M. A., "Quantum phase magnification," *Science* **352**, 1552–1555 (2016).

[16] Linnemann, D., Strobel, H., Muessel, W., Schulz, J., Lewis-Swan, R. J., Kheruntsyan, K. V., and Oberthaler, M. K., "Quantum-enhanced sensing based on time reversal of nonlinear dynamics," *Physical Review Letters* **117**, 013001 (2016).

[17] Bollinger, J. J., Itano, W. M., Wineland, D. J., and Heinzen, D. J., "Optimal frequency measurements with maximally correlated states," *Physical Review A* **54**, R4649(R) (1996).

[18] Kitagawa, M. and Ueda, M., "Squeezed spin states," *Physical Review A* **47**, 5138–5143 (1993).

[19] Leroux, I. D., Schleier-Smith, M. H., and Vuletić, V., "Implementation of cavity squeezing of a collective atomic spin," *Phys. Rev. Lett.* **104**, 073602 (2010).

[20] Bohnet, J. G., Sawyer, B. C., Britton, J. W., Wall, M. L., Rey, A. M., Foss-Feig, M., and Bollinger, J. J., "Quantum spin dynamics and entanglement generation with hundreds of trapped ions," *Science* **352**, 1297–1301 (2016).

[21] Schleier-Smith, M. H., Leroux, I. D., and Vuletić, V., "States of an ensemble of two-level atoms with reduced quantum uncertainty," *Physical Review Letters* **104**, 073604 (Feb 2010).

[22] Strobel, H., Muessel, W., Linnemann, D., Zibold, T., Hume, D. B., Pezzè, L., Smerzi, A., and Oberthaler, M. K., "Fisher information and entanglement of non-gaussian spin states," *Science* **345**, 424–427 (2014).

[23] Apellaniz, I., Lücke, B., Peise, J., Klempt, C., and Tóth, G., "Detecting metrologically useful entanglement in the vicinity of dicke states," *New Journal of Physics* **17**, 083027 (2013).

[24] Kessler, E., Kómár, P., Bishof, M., Jiang, L., Sørensen, A., Ye, J., and Lukin, M., "Heisenberg-limited atom clocks based on entangled qubits," *Physical Review Letters* **112**, 190403 (2014).

[25] Braunstein, S. L. and Caves, C. M., "Statistical distance and the geometry of quantum states," *Physical Review Letters* **72**, 3439–3443 (1994).

[26] Hyllus, P., Laskowski, W., Roland Krischek, C. S., Wieczorek, W., Weinfurter, H., Pezzè, L., and Smerzi, A., "Fisher information and multiparticle entanglement," *Physical Review A* **85**, 022321 (2012).

[27] Gärttner, M., Bohnet, J. G., Safavi-Naini, A., Wall, M. L., Bollinger, J. J., and Rey, A. M., "Measuring out-of-time-order correlations and multiple quantum spectra in a trapped ion quantum magnet," *arXiv:1608.08938 [quant-ph]* (2016).

[28] Gil, L., Mukherjee, R., Bridge, E., Jones, M., and Pohl, T., "Spin squeezing in a Rydberg lattice clock," *Physical Review Letters* **112**, 103601 (2014).